DOI:10.1002/ejic.201500057

Room-Temperature Hydrogenation of Citral Catalyzed by Palladium–Silver Nanocrystals Supported on SnO_2

Shuo Wang,[a,b] Rongan Shen,[b] Zheng Chen,[b] Jiaxi Wang,*[a]
Dingsheng Wang,*[b] and Yadong Li[b]

Keywords: Heterogeneous catalysis / Nanocrystals / Hydrogenation / Palladium / Silver / Tin

We have developed two strategies to optimize Pd catalysts. On one hand, Ag was introduced into Pd and then they were applied to the selective hydrogenation of citral under mild conditions. The addition of metallic Ag could tune the selectivity of Pd and made it suitable for the selective hydrogenation of the conjugated double bond. The selectivity of citronellal increased from 0 (for Pd/C and $Pd_{0.7}Ag_{0.3}$/C) to 96 % (for $Pd_{0.4}Ag_{0.6}$/C) as the Ag content increased. On the other hand, the addition of SnO_2 made the Pd catalysts more inclined to activate the C=O bond and gave better performance for the hydrogenation of the conjugated double bond compared with the corresponding Pd–Ag catalysts. The selectivity of citronellal increased from 0 (for $Pd_{0.7}Ag_{0.3}$/C) to 76 % (for $Pd_{0.7}Ag_{0.3}$–SnO_2/C was used) after the addition of SnO_2. On the basis of these results, we developed a catalyst ($Pd_{0.6}Ag_{0.4}$–SnO_2/C) with the best catalytic performance for the selective hydrogenation of citral (the conversion of citral reached 99 %, and the selectivity was up to 96 %).

Introduction

The selective hydrogenation of α,β-unsaturated aldehydes and ketones, such as acrolein, methacrolein, crotonaldehyde, *E*-cinnamaldehyde, citral, and benzalacetone, is an important step in the preparation of different kinds of materials and intermediates in fine chemistry.[1,2] Citral is one of the major components of the essential oils from various plants, including lemon myrtle, litsea citrate, litsea cubeba, and lemon.[3–5] Citral has a conjugated double bond (C=C), an isolated double bond (C=C), and a carbonyl group (C=O).[6,7] The reaction pathways for the hydrogenation of citral are complicated and give various products such as citronellal (CAL), citronellol, geraniol, nerol, menthol, and others through the hydrogenation of the C=C and C=O bonds (Scheme 1). Therefore, it is challenging to control the selectivity of the hydrogenation of citral.

Catalysts based on palladium are commonly used for the hydrogenation of carbon–carbon multiple bonds in various kinds of substrate.[8–11] Palladium catalysts have a higher ability to activate carbon–carbon multiple bonds than other noble metals such as Pt, Ru, and Rh. There have been several previous reports of the selective hydrogenation of citral to citronellal over Pd catalysts through the tuning of the reaction conditions[12–14] and the selection of different supports, including Al_2O_3, zeolite, $CaCO_3$, TiO_2, and sepiolite.[15–18] However, the selectivities to the desired products over these catalysts are not promising, likely because of the poor selectivity of Pd for the hydrogenation of C=C and C=O.

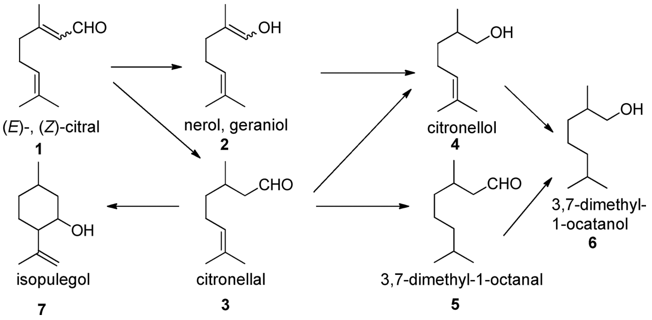

Scheme 1. Pathways for the hydrogenation of citral.

In recent decades, bimetallic nanoparticles (BNPs) have attracted passionate attention.[19–24] They have received steadily growing interest and have been widely applied to catalysis. They exhibit better catalytic performance (especially for activity and selectivity) than that of monometallic nanoparticles (NPs).[25,26] The catalytic performance of BNPs is associated with their composition because each metal in the BNPs can tune the electronic state of the catalytically active component.[27]

Herein, we introduced another metal (Ag) to tune the electronic structure of Pd and make it suitable for the formation of citronellal by the selective hydrogenation of

---

[a] School of Chemical Engineering, Hebei University of Technology,
Tianjin 300130, P. R. China
E-mail: wangjiaxi@hebut.edu.cn
http://www.hebut.edu.cn/
[b] Department of Chemistry, Tsinghua University,
Beijing 100084, P. R. China
E-mail: wangdingsheng@mail.tsinghua.edu.cn
http://www.tsinghua.edu.cn/

Supporting information for this article is available on the WWW under http://dx.doi.org/10.1002/ejic.201500057.

citral. Furthermore, the addition of SnO_2 could improve the reactivity of the conjugated double bond. The morphologies, phase structures, and chemical composition were studied by transmission electron microscopy (TEM), energy dispersive X-ray (EDX) spectroscopy, powder X-ray diffraction (XRD), X-ray photoelectron spectroscopy (XPS), and FTIR spectroscopy. The hydrogenation of citral was performed under a H_2 balloon at room temperature (25 °C). The possible mechanism was also studied.

Results and Discussion

In the synthesis of Pd_xAg_{1-x} BNPs, $Pd(acac)_2$ (acac = acetylacetonate) and $AgOOCCF_3$ (silver trifluoroacetate) were used as the precursors. Oleylamine (OAm) was used as the solvent and surfactant. Both of the precursors were dissolved in OAm and oleic acid at 60 °C and reduced by borane–*tert*-butylamine. The transmission electron microscopy (TEM) images of the as-prepared Pd_xAg_{1-x} ($x = 0$–1) BNPs (Figure 1) showed that all of the BNPs were monodisperse particles and had an average size of ca. 3 nm. When $Pd(acac)_2$ was used as the only precursor, Pd NPs with a particles size of ca. 3 nm (Figure S1a in the Supporting Information) were obtained; when $AgOOCCF_3$ was used as the only precursor, Ag NPs with a particles size of ca. 8 nm (Figure S1b) were produced.

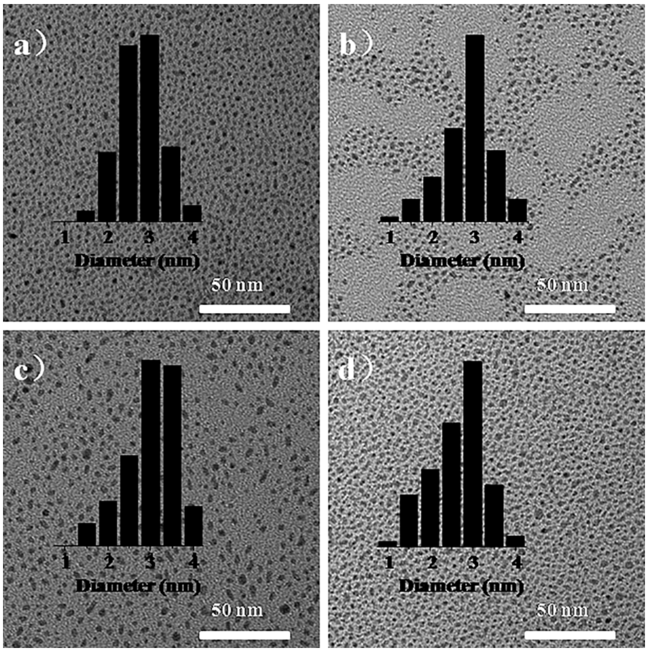

Figure 1. TEM images of Pd_xAg_{1-x} ($x = 0$–1) NPs: (a) $Pd_{0.7}Ag_{0.3}$, (b) $Pd_{0.6}Ag_{0.4}$, (c) $Pd_{0.5}Ag_{0.5}$, and (d) $Pd_{0.4}Ag_{0.6}$.

The powder X-ray diffraction (XRD) patterns of the as-prepared Pd_xAg_{1-x} ($x = 0$–1) BNPs are shown in Figure 2. The shift of the (111) diffraction peak corresponding to Pd (JCPDS 65-6174) towards that of Ag (JCPDS 65-2871) as the Ag content increases demonstrates the formation of the bimetallic structure of the obtained NPs.

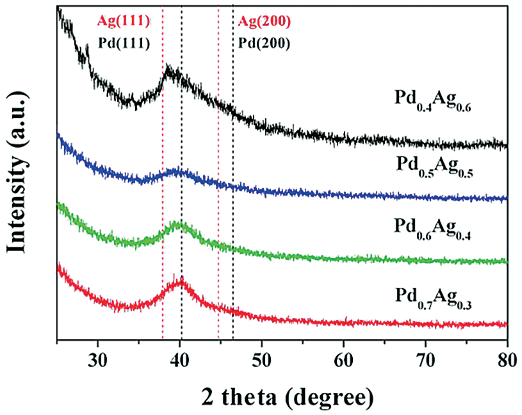

Figure 2. XRD patterns of Pd_xAg_{1-x}/C ($x = 0$–1).

X-ray photoelectron spectroscopy (XPS) showed the binding energy peaks of Pd and Ag in the products (Figure 3, a and b). The strong Ag $3d_{5/2}$ signals were located at 367.8–367.9 eV, which are lower than that of the pure metal (368.3 eV); the dominant peaks at 335.4–335.6 eV were attributed to Pd $3d_{5/2}$. The Pd peaks only shifted when there were enough Ag atoms to sufficiently disturb the Pd–Pd bonding.[28] In addition, energy dispersive X-ray (EDX) spectroscopy (Figure S2) and inductively coupled plasma atomic emission spectrometry (ICP-AES) showed that the exact Pd/Ag molar ratios of the synthesized Pd_xAg_{1-x} BNPs were similar to the proportions of their precursors. The Ag-rich surface of the Pd–Ag alloy could be also detected by XPS and ICP-AES (Table S1).

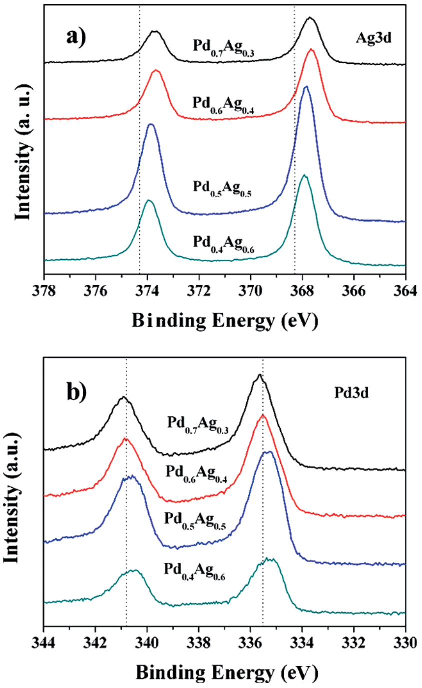

Figure 3. XPS spectra of Pd_xAg_{1-x}.

The pathways for the hydrogenation of citral are shown in Scheme 1. Citronellal (**3**) and 3,7-dimethyl-1-octanal (**5**) were the two principal products in our system. The BNPs were loaded on active carbon before use (details are provided in the Experimental Section). The catalytic performance of the as-synthesized Pd_xAg_{1-x}/C was evaluated in the selective hydrogenation of citral. The reaction was performed with 2-propanol as the solvent at room temperature and under normal pressure (Table 1). Two benchmark catalysts, commercial Pd/C and home-made Pd/C were initially tested. They had high activity but low selectivity for **3** in the present system (Table 1, Entries 1 and 2). In addition, as the ratio of Ag increased, the selectivity for **3** increased from 0 to 96% (Table 1, Entries 3–6). The activity of the Pd_xAg_{1-x} catalysts began to decline when the Pd/Ag molar ratio reached 2:3, and Ag particles were inactive in this reaction system.

Table 1. Hydrogenation of citral catalyzed by Pd_xAg_{1-x}–SnO_2/C.[a]

Entry	Catalyst	Time [h]	Conv. [%]	Selectivity [%][b]		
				3	5	Others[c]
1	commercial Pd/C	12	99		96	4
2	home-made Pd/C	12	99		94	6
3	$Pd_{0.7}Ag_{0.3}$/C	12	99	–	85	15
4	$Pd_{0.6}Ag_{0.4}$/C	12	99	8	77	15
5	$Pd_{0.5}Ag_{0.5}$/C	12	99	81	13	6
6	$Pd_{0.4}Ag_{0.6}$/C	12	56	96	–	4
7	Ag/C	12	–	–	–	–
8	Pd–SnO_2/C	12	99	4	92	4
9	$Pd_{0.7}Ag_{0.3}$–SnO_2/C	12	99	76	19	5
10	$Pd_{0.6}Ag_{0.4}$–SnO_2/C	12	99	96	2	2
11	$Pd_{0.5}Ag_{0.5}$–SnO_2/C	12	64	98	–	2
12	$Pd_{0.4}Ag_{0.6}$–SnO_2/C	12	12	98	–	2
13	SnO_2/C	12	–	–	–	–

[a] Reaction conditions: substrate **1** (1 mmol), catalyst (0.8 mol-% based on Pd) in 2-propanol (3 mL) at room temperature, H_2 balloon. [b] The conversion and selectivity were analyzed by GC, and *n*-dodecane was used as the internal standard. [c] Others including but not limited to **2**, **4**, **6**, and **7** produced by the hydrogenation of citral.

Various ratios of Pd and Ag catalysts gave different selectivity for citronellal, and this was ascribed to the following two factors: Firstly, the conjugated C=C bond is easier to activate than the isolated C=C bond because of the delocalization of electrons in the conjugated C=C–C=O bonds.[29] Secondly, as the Ag atoms practically did not adsorb hydrogen, the addition of Ag to Pd may change the structure of the Pd particles and lead to a decreased quantity of absorbed hydrogen on the Pd–Ag catalysts.[30] Therefore, the Pd–Ag catalysts exhibited decreased selectivity for the isolated C=C bond and enhanced selectivity to citronellal.

Under these conditions, the activity and selectivity could not increase at the same time. Thus, we introduced SnO_2 colloid as a promoter of the Pd_xAg_{1-x} BNPs, (the details are provided in the Experimental Section). The TEM image of $Pd_{0.6}Ag_{0.4}$–SnO_2 (Figure S1) showed that the $Pd_{0.6}Ag_{0.4}$ BNPs were well supported on SnO_2. The XRD patterns also revealed that the intensity of Pd_xAg_{1-x}–SnO_2 supported on active carbon (Figure S3 in the Supporting Information) was quite strong compared with that of Pd_xAg_{1-x} BNPs. The amount of Pd–Ag BNPs loaded on the surface of SnO_2 was detected by ICP-AES (Table S1).

The presence of SnO_2 species could provide positive electron-donating effects from the precious metal atoms to the promoters, and this effect could lead to the C=C bond activation decreasing and C=O bond activation increasing.[31,32] Therefore, compared with the corresponding Pd–Ag catalysts, it is easier for Pd_xAg_{1-x} supported on SnO_2 to activate the C=O bond of citral, and the conjugated C=C bond adjacent to the C=O bond was more readily activated than the isolated C=C bond far from the C=O bond. On account of the constraints of the Pd–Ag catalysts, there was a small amount of saturated and unsaturated alcohol. Consequently, compound **3** could be obtained with a conversion of 99% and selectivity of 96% with $Pd_{0.6}Ag_{0.4}$–SnO_2/C as the catalyst (Table 1, Entry 10).

Next, we investigated the possible reaction paths for the reduction of citral to citronellal and other products. The influence of the catalyst loading and the initial concentration of citral on the conversion and selectivity were studied with Pd_xAg_{1-x}/C and Pd_xAg_{1-x}–SnO_2/C as the catalysts. A series of conversion and selectivity versus time curves were plotted (Figure S4). The conversion and selectivity versus time for the $Pd_{0.6}Ag_{0.4}$/C catalyst are shown in Figure 4 (a), and the conversion of citral reach almost 99% within 40 min, whereas it took nearly 12 h with the $Pd_{0.6}Ag_{0.4}$–SnO_2/C catalyst (Figure 4, b). However, when $Pd_{0.6}Ag_{0.4}$–SnO_2/C was used, the selectivity of citronellal remained

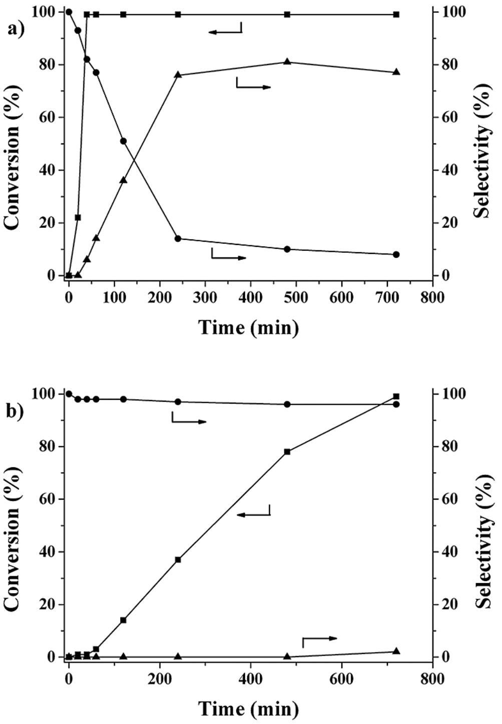

Figure 4. Conversion and selectivity versus time for the hydrogenation of citral with $Pd_{1-x}Ag_x$–SnO_2 (x = 0–1) catalysts: (a) $Pd_{0.6}Ag_{0.4}$/C and (b) $Pd_{0.6}Ag_{0.4}$–SnO_2/C; ■ conversion of citral (**1**), ● selectivity of CAL (**3**), ▲ selectivity of DCAL (**5**). Reaction conditions: citral (1 mmol), catalyst (0.8 mol-% based on Pd) in 2-propanol (3 mL) at room temperature under a H_2 balloon.

above 95% as the reaction proceed to 99% conversion. On the contrary, when $Pd_{0.6}Ag_{0.4}/C$ was used as the catalyst, the selectivity of citronellal began to decrease after 20 min and declined to less than 10% after 12 h. The turnover frequencies (TOFs, Table S3) decreased as the Ag content increased or as SnO_2 was added. Furthermore, we could obtain citronellal with high selectivity under mild conditions compared with those reported previously (Table S4).

Finally, to study the stability of the $Pd_{0.6}Ag_{0.4}–SnO_2/C$ catalyst, it was recycled in the hydrogenation of citral under the previous conditions after centrifugation and filtration (Figure 5). The results showed that the catalyst is still highly active (97% conversion of citral) and selective (96% citronellal) after four cycles. TEM (Figure S5) showed that the $Pd_{0.6}Ag_{0.4}–SnO_2/C$ catalyst had no clear changes after use. In the FTIR spectra (Figure S6 in the Supporting Information), the peaks at $\tilde{\nu}$ = 2920 and 2877 cm^{-1} were assigned to the symmetric methylene stretches and the antisymmetric methyl group; therefore, we concluded that the hydrophobic long chain ligand had capped the catalyst. The COOH modes at $\tilde{\nu}$ = 3431 and 1601 cm^{-1} indicated the anchoring of oleic acid. The weakening of the peaks showed that the excess ligand on the surface of the Pd–Ag catalyst had decreased after four cycles, and this may enhance the reactivity of the catalyst.

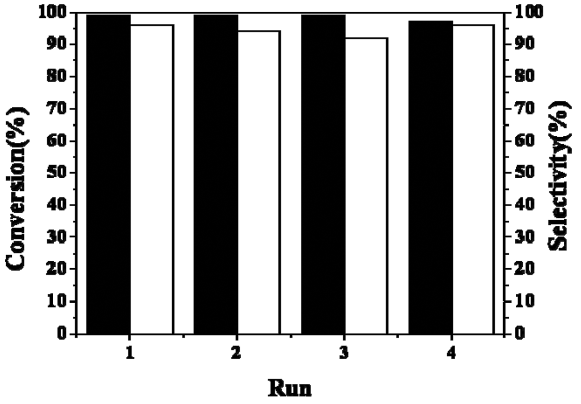

Figure 5. Recycling experiment of $Pd_{0.6}Ag_{0.4}–SnO_2/C$ catalyst in the hydrogenation of citral for 12 h.

Conclusions

We successfully prepared a selective bimetallic $Pd_{0.6}Ag_{0.4}–SnO_2/C$ catalyst for the hydrogenation of citral to citronellal. The conversion reached 99%, and the selectivity for citronellal reached 96%. For the Pd catalyst, either alloying with Ag or support on SnO_2 improved its selectivity to citronellal. This result implies that the performance of an active metal catalyst can be tuned by the introduction of another metal. Transition metal oxide (TMO) supports also effectively improved the performance of noble metal catalysts. We anticipate that such methods could be extended to the development of specific heterogeneous catalysts for other important reactions.

Experimental Section

Chemicals: Commercial Pd/C, $Pd(acac)_2$ and tin(IV) oxide (15% in H_2O colloidal dispersion) were obtained from Alfa Aesar, silver trifluoroacetate and oleylamine (OAm) were purchased from J&K Chemical, and activated carbon was obtained from TCI. Analytical-grade ethanol, cyclohexane, and oleic acid were purchased from Beijing Chemical Reagents. All of the chemicals were used without further purification.

Synthesis: In a typical preparation of $Pd_{0.5}Ag_{0.5}$ nanocrystals, silver trifluoroacetate (14.5 mg) and $Pd(acac)_2$ (20 mg) were dissolved in OAm (1 mL) and injected into OAm (5 mL) and oleic acid (200 µL) at 60 °C with vigorous stirring for 10 min. Then, a solution of borane–*tert*-butylamine (100 mg, 1.15 mmol) in OAm (1 mL) was added quickly into the previous solution, and the reaction mixture immediately turned black. After 5 min, the flask was heated to 90 °C for a further 1 h. After cooling to room temperature, the solution was washed with ethanol (40mL × 3) and then dispersed in cyclohexane for future use.

The procedure for the typical preparation of $Pd_{0.5}Ag_{0.5}–SnO_2$ was the same as that for the synthesis of Pd–Ag BNPs, and oleic acid was used as the stabilizer for SnO_2. After 1 h, tin(IV) oxide (250 µL, 37.5 mg, 15% in H_2O colloidal dispersion) was added dropwise into the reaction mixture with vigorous stirring for a further 1 h at 120 °C. After cooling to room temperature, the solution was washed with ethanol (40mL × 3) and then dispersed in cyclohexane for future use.

For the preparation of Pd_xAg_{1-x}/C $(0 < x < 1)$ and $Pd_xAg_{1-x}–SnO_2/C$ $(0 < x < 1)$ catalysts, the activated carbon was added into the dispersions of Pd_xAg_{1-x} $(0 < x < 1)$ and $Pd_xAg_{1-x}–SnO_2$ $(0 < x 1)$ at a loading of 3 wt.-% (based on Pd and Ag, the actual content is shown in Table S2), and the mixtures were stirred overnight. The catalysts were obtained through centrifugation and drying under vacuum.

Characterization: The powder XRD patterns were recorded with a Bruker D8 ADVANCE X-ray powder diffractometer with Cu-K_α radiation (λ = 1.5406 Å). The sample compositions were determined by ICP-AES, and the particle size and dispersion were investigated with a Hitachi H-800 transmission electron microscope (TEM). The X-ray photoelectron spectroscopy (XPS) was conducted with a Thermo Fisher ESCALAB 250Xi spectrometer equipped with a monochromatic Al X-ray source.

Catalytic Properties: For a typical run, citral (1 mmol) and Pd_xAg_{1-x}/C or $Pd_xAg_{1-x}–SnO_2/C$ catalyst (0.8 mol-% of citral based on Pd and Ag) were placed in a 10 mL flask with 2-propanol (3 mL) as the solvent. A H_2 balloon was introduced after the flask was purged three times with H_2. The reaction was performed at room temperature (25 °C) for the specified time. Liquid samples were analyzed by gas chromatography with a Thermo Finnigan chromatograph equipped with a flame ionization detector and a DB-WAX capillary column (J&W, 30 m, 0.25 mm i.d.) with nitrogen as the carrier gas.

Supporting Information: (see footnote on the first page of this article): Compositions of the as-prepared catalysts by ICP-AES and XPS (Tables S1 and S2); TEM images of Pd, Ag, and $Pd_{0.6}Ag_{0.4}–SnO_2$ (Figure S1); XRD patterns of as-prepared $Pd_xAg_{1-x}–SnO_2/C$ (x = 0–1; Figure S2); EDX spectra of as-prepared Pd_xAg_{1-x} (x = 0–1; Figure S3); and conversion and selectivity versus time in the hydrogenation of citral Pd_xAg_{1-x}/C (x = 0–1) and $Pd_xAg_{1-x}–SnO_2/C$ (x = 0–1) catalysts (Figure S4).

Acknowledgments

Financial support of this work by the State Key Project of Fundamental Research for Nanoscience and Nanotechnology (grant numbers 2011CB932401, 2011CBA00500, 2012CB224802), the Foundation for the Author of National Excellent Doctoral Dissertation of P. R. China (201321), the Specialized Research Fund for the Doctoral Program of Higher Education (20130002120013), and the National Natural Science Foundation of China (NSFC) (21231005, 21471089, 21322107) is gratefully acknowledged.

---

[1] L. N. Protasova, E. V. Rebrov, H. E. Skelton, A. E. H. Wheatley, J. C. Schouten, *Appl. Catal. A* **2011**, *399*, 12–21.

[2] N. M. Bertero, A. F. Trasarti, B. Moraweck, A. Borgna, A. J. Marchi, *Appl. Catal. A* **2009**, *358*, 32–41.

[3] E. Salminen, P. Virtanen, K. Kordás, J. Mikkola, *Catal. Today* **2012**, *196*, 126–131.

[4] J. K. Kim, C. S. Kang, J. K. Lee, Y. R. Kim, H. Y. Han, H. K. Yun, *Entomol. Res.* **2005**, *35*, 117–120.

[5] A. Stolle, T. Gallert, C. Schmöger, B. Ondruschka, *RSC Adv.* **2013**, *3*, 2112–2153.

[6] H. Surburg, J. Panten, *Common Fragrance and Flavor Materials*, Wiley-VCH, Weinheim, Germany, **2006**.

[7] U. K. Singh, M. A. Vannice, *J. Catal.* **2001**, *199*, 73–84.

[8] M. Armbrüster, G. Wowsnick, M. Friedrich, M. Heggen, R. Cardoso-Gil, *J. Am. Chem. Soc.* **2011**, *133*, 9112–9118.

[9] K. Han, H. Zuo, Z. Zhu, G. Cao, C. Lu, Y. Wang, *Ind. Eng. Chem. Res.* **2013**, *52*, 17750–17759.

[10] A. Jung, A. Jess, T. Schubert, W. Schütz, *Appl. Catal. A* **2009**, *362*, 95–105.

[11] P. A. Robles-Dutenhefner, M. G. Speziali, E. M. B. Sousa, E. N. dos Santos, E. V. Gusevskaya, *Appl. Catal. A* **2005**, *295*, 52–58.

[12] M. A. Aramendía, V. Borau, C. Jimenez, J. M. Marinas, A. Porras, F. J. Urbano, *J. Catal.* **1997**, *172*, 46–54.

[13] C. Schmöger, A. Stolle, W. Bonrath, B. Ondruschka, T. Keller, K. D. Jandt, *ChemSusChem* **2009**, *2*, 77–82.

[14] J. Zhu, M. Li, M. Lu, J. Zhu, *Catal. Sci. Technol.* **2013**, *3*, 737–744.

[15] M. Steffan, M. Lucas, A. Brandner, M. Wollny, N. Oldenburg, P. Claus, *Chem. Ing. Tech.* **2006**, *78*, 923–929.

[16] C. Schmöger, T. Gallert, A. Stolle, B. Ondruschka, W. Bonrath, *Chem. Eng. Technol.* **2011**, *34*, 445–451.

[17] S. Yilmaz, S. Ucar, L. Artok, H. Gulec, *Appl. Catal. A* **2005**, *287*, 261–266.

[18] V. Satagopan, S. B. Chandalia, *J. Chem. Technol. Biotechnol.* **1994**, *59*, 257–263.

[19] V. R. Stamenkovic, B. Fowler, B. S. Mun, G. Wang, P. N. Ross, C. A. Lucas, N. M. Markovic, *Science* **2007**, *315*, 493–497.

[20] S. Guo, S. Sun, *J. Am. Chem. Soc.* **2012**, *134*, 2492–2495.

[21] B. Yoon, C. M. Wai, *J. Am. Chem. Soc.* **2005**, *127*, 17174–17175.

[22] N. A. Dehm, X. Zhang, J. M. Buriak, *Inorg. Chem.* **2010**, *49*, 2706–2714.

[23] Z. Niu, D. Wang, R. Yu, Q. Peng, Y. Li, *Chem. Sci.* **2012**, *3*, 1925–1929.

[24] Q. Zhang, X. Guo, Z. Liang, J. Zeng, J. Yang, S. Liao, *Nano Res.* **2013**, *6*, 571–580.

[25] L. Li, Z. Niu, S. Cai, Y. Zhi, H. Li, H. Rong, L. Liu, L. Liu, W. He, Y. Li, *Chem. Commun.* **2013**, *49*, 6843–6845.

[26] S. Cai, H. Duan, H. Rong, D. Wang, L. Li, W. He, Y. Li, *Acs Catal.* **2013**, *3*, 608–612.

[27] H. Rong, S. Cai, Z. Niu, Y. Li, *Acs Catal.* **2013**, *3*, 1560–1563.

[28] D. A. Slanac, W. G. Hardin, K. P. Johnston, K. J. J. Stevenson, *J. Am. Chem. Soc.* **2012**, *134*, 9812–9819.

[29] R. Liu, Y. Yu, K. Yoshida, G. Li, H. Jiang, M. Zhang, F. Zhao, S. Fujita, M. Arai, *J. Catal.* **2010**, *269*, 191–200.

[30] Q. Zhang, J. Li, X. Liu, Q. Zhu, *Appl. Catal. A* **2000**, *197*, 221–228.

[31] K. Liberková, R. Touroude, *J. Mol. Catal. A* **2002**, *180*, 221–230.

[32] A. Vicente, G. Lafaye, C. Especel, P. Marécot, C. Williams, *J. Catal.* **2011**, *283*, 133–142.

Received: January 21, 2015

Supported Bimetallic Catalysts

S. Wang, R. Shen, Z. Chen, J. Wang,* D. Wang,* Y. Li 1–6

Room-Temperature Hydrogenation of Citral Catalyzed by Palladium–Silver Nanocrystals Supported on SnO_2

Keywords: Heterogeneous catalysis / Nanocrystals / Hydrogenation / Palladium / Silver / Tin

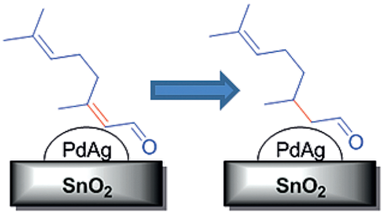

We have developed two strategies to optimize Pd catalysts for the selective hydrogenation of citral and exploited a catalyst ($Pd_{0.6}Ag_{0.4}$–SnO_2/C) with the best catalytic performance (the conversion of citral reached 99%, and the selectivity was up to 96%).